Journal of Holistic Integrative Pharmacy 4 (2023) 259–271

Contents lists available at ScienceDirect

Journal of Holistic Integrative Pharmacy

journal homepage: www.keaipublishing.com/en/journals/journal-of-holistic-integrative-pharmacy

Combining single-cell RNA sequencing data and network pharmacology to explore the mechanism of action of Dayuan Yin in the treatment of acute lung injury

Lei Zhang *, Wei Zhu, Zepeng Zhang, Yu Huang

Kunshan Hospital of Traditional Chinese Medicine, Kunshan, 215300, China

ARTICLE INFO

Keywords:
Single cell sequencing
Network pharmacology
Molecular docking
Dayuan yin
Acute lung injury

ABSTRACT

Background: This study aimed to analyze the usefulness of combined single-cell RNA sequencing data and network pharmacology in understanding the molecular regulation mechanism of Dayuan Yin (DYY) in acute lung injury (ALI).

Methods: The single-cell ALI dataset GSE224938 was acquired from the Gene Expression Database and cellular heterogeneity was examined using the Seurat software package. Differential expression analysis was conducted using the R software to identify genes with significant expression differences. The active constituents and therapeutic targets of DYY were acquired from the Traditional Chinese Medicine Systems Pharmacology (TCMSP) database. Subsequently, the protein-protein interaction (PPI) networks, gene ontology (GO), and Kyoto Encyclopedia of Genes and Genomes (KEGG) were employed to analyze the key targets. A visual network depicting the interaction between compounds, targets, and pathways was constructed, and the CytoNCA plug-in was utilized to identify core targets. The active component-core target relationship was validated using MOE, AutoDockTools, AutoDockVina, and other software. Finally, a preliminary experiment was conducted using the lipopolysaccharide-induced acute lung injury (ALI) rat model.

Results: In total, 5243 significantly differentially expressed genes were identified in ALI, and 260 genes were identified as DYY targets. Then, 81 target genes were identified at the intersection between drugs and diseases. The identified core target genes included PIK3R1, IL-1β, IL-6, ICAM1, and CCL2. GO analysis was mainly involved in cellular inflammatory response, dual regulation of cell apoptosis, and coordinated migration. KEGG analysis showed enrichment in inflammatory pathways. The major active components were well connected with IL-1β. DYY could significantly reduce the phosphorylation expression of PI3K, Akt, and NF-κBp65 in the lung tissue of ALI rats, and regulated the activation of related inflammatory cells.

Conclusions: We successfully screened the potential active ingredients of DYY for the treatment of ALI. In addition, in vivo experiments preliminarily verified the predictions of network pharmacology, showing that DYY can inhibit the PI3K/Akt/NF−KB signaling pathway, reduce cytokine release and regulate the number of inflammatory cells, providing an alternative for ALI treatment.

1. Introduction

Acute lung injury (ALI) is a prevalent inflammatory disorder characterized by diffuse alveolar damage and pulmonary edema. Inadequate management of ALI can result in the development of acute respiratory distress syndrome (ARDS), which is linked to considerable mortality and disability.[1,2] Prior research has established that the excessive activation of inflammatory cells and the overproduction of pro-inflammatory mediators can elicit oxidative stress in the lungs, heighten the permeability of pulmonary endothelial cells, and introduce substantial quantities of protein-rich substances into bronchial and alveolar cavities, thereby precipitating pulmonary edema.[3]

At present, there is a lack of a recommended specific pharmaceutical intervention for the treatment of ALI that exclusively targets the underlying etiology of the ailment. Conventional therapeutic approaches encompass the utilization of antioxidants, glucocorticoids, and anti-inflammatory agents. Nevertheless, there exists a pressing demand for pharmaceutical interventions capable of effectively curing or reversing

* Corresponding author. Kunshan Hospital of Traditional Chinese Medicine, 60 Changyang Branch Road, 215300, China.
E-mail address: zhl0320@163.com (L. Zhang).

https://doi.org/10.1016/j.jhip.2024.01.002
Received 29 November 2023; Received in revised form 10 January 2024; Accepted 10 January 2024

the progression of the disease.[4–6] Traditional Chinese medicine (TCM) has garnered aextensive utilization over millennia for the management of respiratory disorders. Scholars have not only revealed new potential components for treating ALI, but also studied its molecular mechanisms from different perspectives, confirming its overall therapeutic advantages[7] and reliably evaluating its safety,[8] which can be used as an aeffective supplement to the conventional treatment for ALI. In TCM, ALI belongs to the category of "dyspnea syndrome".[7] It is believed that it is mostly caused by the invasion of external pathogens, such as cold and dampness, as well as internal injuries such as dietary habits, emotional disturbances, and chronic illnesses. "Heat, toxin, phlegm, and blood stasis" run through the whole process of ALI, and inflammatory disorder is the main reaction characteristic of ALI.[9] Dayuan Yin (DYY) is composed of *Magnolia officinalis*, *Amomum tsao-ko*, *Areca nut*, *Scutellaria baicalensis*, *Anemarrhena asphodeloides Bunge, Radix paeoniae Alba* and *Radix Glycyrrhizae*, it has the effect of clearing heat and detoxification, and it has been confirmed to have multiple targets and pathways. It is commonly used in clinical treatment of various types of fever and inflammation.[10] Its single ingredient has been proved to be effective in improving the symptoms of ALI.[11–13] In addition, inhibition of the PI3K/Akt signaling pathway has been demonstrated to have a protective effect against LPS-induced ALI.[14] However, the overall role of DYY and its relationship with this signaling pathway remain unclear. Based on large-scale databases, network pharmacology has upgraded the traditional "one target–one drug" research model to a modern approach of "multiple components–multiple targets–multiple pathways", which is conducive to elucidate the mechanism of drug action from the overall perspective and provides a powerful tool for the systematic study of Chinese medicine prescriptions.[15,16] However, the aforementioned is intrinsically linked to the assistance provided by omics technology. By incorporating single-cell sequencing data, this investigation employed network pharmacology to amalgamate information analysis pertaining to the "cell" dimension, thereby facilitating precise identification of potential target genes. Additionally, it enhances comprehension of the alterations occurring in crucial inflammatory cells in vivo, thereby infusing novel vigor into the prospective utilization of single-cell sequencing technology to comprehensively and accurately elucidate the mechanisms of action underlying diverse lung cell types and their subtypes in therapeutic interventions.[17]

This study integrated single-cell sequencing data mining, network pharmacology, and molecular docking techniques to systematically analyze the potential active components, action targets, and regulatory pathways of DYY in the treatment of ALI, which were verified by molecular simulation. Therefore, a rat ALI model was established to preliminarily verify this speculation.

2. Materials and methods

2.1. Download and analysis of RNA sequencing (RNA-seq) data

The single-cell dataset GSE224938[18] for ALI, which was obtained from the Gene Expression Omnibus (GEO; https://www.ncbi.nlm.nih.gov/geo/gds). Seurat 5.0 (https://satijalab.org/seurat/), was used for the quality control of the single-cell RNA sequencing data. The NormalizeData function was used to standardize the data of each sample, whereas the Find-VariableFeatures function was used to calculate the coefficient of variation (standard deviation) of genes between cells, which enabled the identification of genes with significant differences between cells to identify cell types later. A principal component analysis (PCA) was performed to reduce the dimensionality of the sample data through the "RunPCA" function. The principal components with $P < 0.05$ were selected, and the Unified Manifold Approximation and Projection algorithm (UMAP) was used to cluster and draw visual maps to better identify the marker genes and cell type of each cluster. Fisher's test was used to analyze the differences in cell types between ALI and control samples.

2.2. Screening of core targets

The chip data were divided into ALI samples and control samples using the R software. The limma package was applied with the threshold of $|\log2\ (\text{foldchange, FC})| > 1$ and corrected $P < 0.05$[19] to obtain the significant differentially expressed genes (DEGs) related to ALI. The top five characteristic genes from both upregulated and downregulated genes were selected to generate heatmaps and volcano plots. Combined with the characteristics of oral administration of DYY, the potential active ingredients of DYY were screened by accessing TCM system pharmacology (TCMSP, https://tcmspw.com/tcmsp.php) and China knowledge Network (https://www.cnki.net/) databases with the criteria of oral bioavailability ≥30 %, drug-likeness ≥0.18, and half-life ≥ 4.[20] Based on the Swiss Target Predictions database (http://www.swisstargetprediction.ch/), the potential targets of the chemical components obtained by the abovementioned screening were extracted with a probability threshold set at > 0. The disease and drug targets were imported into the R software, a Venn diagram was drawn, and the drug–disease intersection targets were screened by mapping.

2.3. Gene ontology (GO) and Kyoto Encyclopedia of Genes and Genomes (KEGG) enrichment analysis

According to the intersection targets submitted by KOBAS3.0 (http://kobas.cbi.pku.edu.cn/index.php) database, biological processes (BP) of GO was filtered under the conditions of "homosapiens" and "$P < 0.05$", then KEGG pathway enrichment analyses was also performed. The WeChat online mapping cloud platform was used to draw an advanced bubble diagram to visualize the results.

2.4. Construction of a PPI network

Target genes were imported into the STRING platform (http://string-db.org/) to construct a protein–protein interaction (PPI) network. This species is restricted to "*Homo sapiens*". The PPI network was then exported to the TSV format file and imported into the Cytoscape3.7.2 software for visualization, and the core target genes of DYY were filtered for treating ALI using the Cytohubba plug-in DMNC algorithm.

2.5. Construction and analysis of components–gene targets–pathway networks

To demonstrate the mechanism of action of DYY in treating ALI more clearly, Cytoscape 3.7.2 (https://www.cytoscape.org/) was utilized to construct a network diagram of active component–gene targets–action pathways, and a degree analysis was performed using the CytoNCA plug-in to identify and predict the major active components of DYY in ALI treatment.

2.6. Molecular docking

Download candidate compositions and target protein structures from the TCMSP database and the PDB database (https://www.rcsb.org/), respectively. The eutectic ligands and water molecules contained in the protein structure were removed, and residue repair and hydrogenation were carried out. Then AutoDockTools1.5.6 was imported to construct docking grid for each target. Finally, the docking was completed by AutodockVina1.2.2 software, and visualization was achieved using MOE software (https://www.chemcomp.com/Products.htm).

2.7. In vivo validation

2.7.1. Drug administration in rats

The SD rats utilized in this study were purchased from the Wuhan Optimal Biotechnology Co., Ltd.(Wuhan, China) [Production number: SCXK(e) 2021–0025; Use number: SYXK(e) 2021–0115]. The rats were

randomly divided into five groups (n = 6): control, model, low, middle, and high dose (3.48, 6.96, 13.92 g/kg) DYY groups with six rats each. Except for the control group, ALI was induced in the remaining four groups of rats by intraperitoneal injection of 10 mg/kg LPS.[21] After 6 h, the treatment groups were orally administered different concentrations of DYY, whereas the control and model groups were administered normal saline continuously for 3 days.

2.7.2. Collection of alveolar lavage fluid and lung tissue

After the rats were killed, the left alveoli were lavaged with pre-cooled phosphate-buffered saline (PBS) for three times, and bronchoalveolar lavage fluid (BALF) was collected.[22] The supernatant after BALF centrifugation was used to determine the level of inflammatory cytokines, and the sediment was used to classify and count inflammatory cells. Meanwhile, the upper lobe of the right lung was isolated for pathological observation, the middle lobe was used to determine the lung wet/dry weight (W/D) ratio, and the lower lobe was used for Western blot analysis.

2.7.3. Calculation of lung W/D value in rats

To reflect the severity of lung injury as a whole, we measured the W/D ratio to directly reflect pulmonary edema, which was then rinsed with pre-cooled normal saline, dried with a filter paper, weighed, and recorded as the wet weight. Overweight lung tissues were then dried to a constant weight in an incubator, and the dry weight was recorded to calculate the W/D ratio.

2.7.4. Observation on pathomorphology of lung tissues

The right upper lobe lung tissue of each rat was fixed with 10 % neutral-buffered formalin for 48 h, dehydrated with ethanol and coated with wax, dehydrated with conventional gradient ethanol paraffin-embedded at 5-μm thickness, dried for 2 h at 60 °C, eluted with gradient ethanol, dewaxed with xylene, and stained with hematoxylin–eosin, sealed with neutral glue, and dried and observed for injuries caused by inflammatory cell infiltration under a light microscope.[23]

2.7.5. Western blot analysis

The protein was extracted after lung tissue lysis and then transferred to PVDF membrane. The total protein concentration was determined according to the instructions of bicinchoninic acid (BCA) protein assay kit. Two hours after Tris-buffered saline with 0.1 % Tween® 20 detergent (TBST) washing, the membrane was sealed with 5 % skimmed milk powder, and p-PI3k (diluted 1:800), *p*-Akt (dilute 1:1000), and p-p65 (dilute 1:1000) polyclonal antibodies were added. The membrane was placed in the refrigerator overnight at 4 °C before being washed with TBST thrice, and horseradish peroxidase conjugated II antibody was added and reacted in a 37 °C shaker for 1 h. Finally, Image-J was used to quantitatively analyze the relative expression levels of each protein. Using GAPDH density as internal control, the gray density of protein bands was normalized.[24]

2.7.6. Detection of inflammatory cytokines and count of inflammatory cells in BALF

To further confirm the effect of inflammatory pathway on the release of inflammatory factors and stimulation of inflammatory cells, we first measured the contents of tumor necrosis factor (TNF)-α, interleukin (IL)-6, and IL-1β in bronchoalveolar lavage fluid. The specific operations were conducted according to the requirements of relevant kits. The lower layer of the BALF was precipitated, resuspended in PBS, and evenly applied to the center of the slide. After drying, the slides were stained with Wright–Giemsa[25] and washed with water for 3 min. After drying, slides were sealed with neutral gum. The numbers of lymphocytes, neutrophils, and macrophages were observed and analyzed under an optical microscope.

2.7.7. Statistical analyses

The data were processed and analyzed using SPSS26.0. We used mean ± standard deviation to express continuous variables, performed an analysis of variance for each group, and the least significant difference-t multiple test was performed between the groups, both with statistical significance of $P < 0.05$ and $P < 0.01$.

3. Results

3.1. Cell dimensionality reduction clustering and annotation results

The filtered samples were subjected to a linear dimensionality reduction using PCA. Subsequently, principal components with a $P < 0.05$ were selected for UMAP clustering analysis. As a result, the normal and model group can be clearly distinguished and marked with different colors (Fig. 1A). After further clustering and annotation, we identified nine cell subsets, including B cells, T cells, dendritic cells, epithelial cells, granulocytes, macrophages, monocytes, neutrophils, and natural killer cells (Fig. 1B). We then visualized the proportion of these nine cell subsets in the control and model groups. Obviously, both B cells and T cells accounted for a large proportion in the control group, but decreased significantly in the LPS group, while the opposite was true in the case of neutrophils (Fig. 1C).

3.2. Acquisition of potential active targets

We compared the gene expression levels in ALI and normal samples to identify DEGs in ALI. Based on the analysis of a series (GSE224938), a volcanic map was drawn according to the screening criteria, and 5243 genes were identified, of which 4181 were upregulated and 1062 were downregulated in ALI (Fig. 2A and B). Meanwhile, the first five differential genes of up-regulated and down-regulated genes in each cell are presented in a heat map (Fig. 2C). According to the selected standard parameters, the main chemical components of the seven types of Chinese herbal medicines were screened from the TCMSP database and literature. After the exclusion of these components, 94 active components were identified (Supplementary Table S1). After obtaining the corresponding SMILES structures of these ingredients from the PubChem database, repeated targets were eliminated by searching the TCMSP target module, 260 potential targets corresponding to the active compounds of DYY were obtained. Next, we intersected the screened differential genes and the obtained component targets, and 81 intersection targets were finally considered as potential targets for DYY therapy in ALI (Fig. 2D–Supplementary Table S2).

3.3. Results of intersection target enrichment analysis

The 81 DYY targets for the ALI treatment were uploaded to the KOBAS database for GO enrichment and KEGG analyses. GO functional annotation analysis revealed that BPs primarily involved in cell signaling pathways mediated by cytokines, response to drugs, positive regulation of cell migration, and inflammatory response, among others. The top 15 items were visualized (Fig. 3A). In addition, we identified the major signaling pathways ranked by p-values, and the KEGG pathway enrichment analysis revealed the top 10 ALI-related signaling pathways (Fig. 3B), including the AGE-RAGE signaling pathway in diabetic complications, HIF-1 signaling pathway, TNF signaling pathway, PI3K-Akt signaling pathway, and Toll-like receptor signaling pathway. These findings suggest that DYY exerts its therapeutic effects on ALI by acting on the abovementioned multiple pathways (Fig. 3C).

3.4. PPI network analysis

In total, 81 intersection targets were uploaded to the STRING database. Human species were selected. The interaction threshold was set at ≥ 0.4, free nodes were hidden, and a PPI network was constructed and

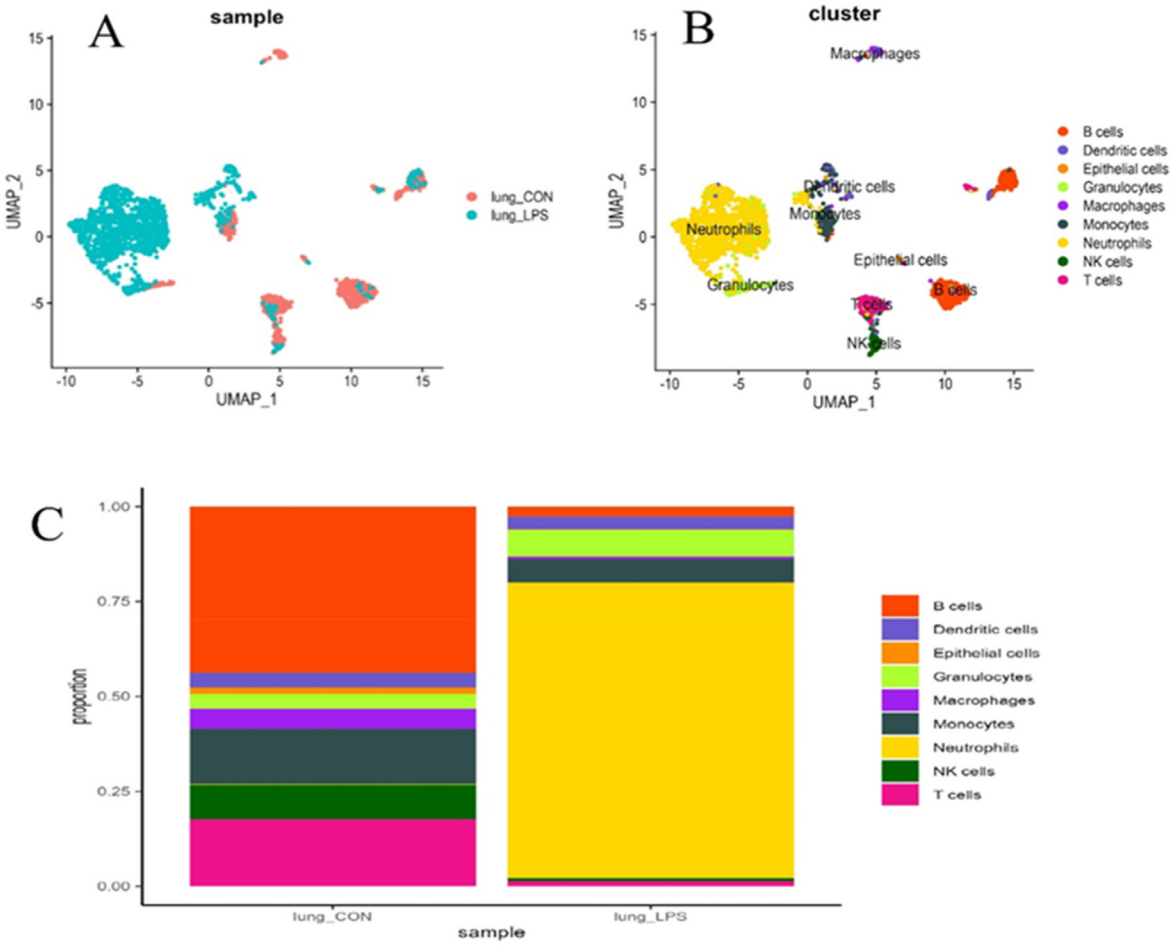

Fig. 1. Dimension reduction clustering and annotation of ALI samples in the GSE224938 dataset. (A) Cluster distribution of cells in the normal and model groups. (B) UMAP of the distribution of each cell subpopulation after annotation. (C) Changes of each cell subpopulation in the normal and model groups.

saved as a TSV format file. A visual network diagram was constructed using the Cytoscape3.7.2 software (Fig. 4A). Analyzed by DMN algorithm of cytoHubba plug-in, sorted by degree value, the first five target genes were identified to be IL-6, IL-1β, PIK3R1, CCL2, and ICAM-1 (Fig. 4B).

3.5. Component–target–pathway network analysis

The "major components-core targets-signal pathways" network of DYY was constructed using Cytoscape3.7.2 software (Fig. 5). We used CytoNCA plug-in for analysis, and finally determined that the key nodes in the network were calycosin (Degree = 30), quercetin (Degree = 24), isorhamnetin (Degree = 17), kaempferol (Degree = 14), and Licochalcone B (Degree = 14) in order of degree value from largest to smallest. These active components may play important roles in the treatment of ALI by using DYY.

3.6. Results of molecular docking

The binding energies between the main active ingredients and core genes were analyzed using molecular docking simulations. Among them, the affinity is the score of the molecular docking result, the smaller the binding energy, the better the binding activity, especially the binding energy < -5.0 kJ mol^{-1} represents the stronger binding activity. The five core components of DYY were calycosin, quercetin, isorhamnetin, kaempferol, and licochalcone B, and the five core targets for treating ALI were IL-6, IL-1β, PIK3R1, CCL2, and ICAM-1. The core components were docked with the core targets. The results revealed that 60 % of the core components were < -3 kJ/mol, and the binding energy between all components and receptors was <0 kJ/mol (Table 1). Each component demonstrated strong binding activity to IL-1β (all <-5 kJ/mol), especially quercetin, which had the strongest binding ability with IL-1β and could also bind well with PIK3R1. Kaempferol and Licochalcone B also demonstrated strong binding to PIK3R1. Finally, the MEO software was used to visualize the molecular docking results (Fig. 6).

3.7. Therapeutic effect and related mechanisms of DYY on ALI rats

3.7.1. Effect of DYY on lung W/D ratio in ALI rats

The results revealed a significant increase ($P < 0.01$) in the lung W/D ratio in the model group compared to that in the control group. After treatment, the lung W/D ratio of the medium- and high-dose DYY groups significantly decreased ($P < 0.05$) compared to that of the model group. (Fig. 7).

3.7.2. Effect of DYY on lung histopathology in rats

The lung tissue morphology and structure of the control group rats were normal, without inflammatory cell infiltration or congestion. Compared with the control group, the model group rats exhibited increased accumulation of inflammatory cells in lung tissue, a significant increase in alveolar space, marked thickening of alveolar walls, and pulmonary capillary bleeding, indicating successful modeling. Lung injury in the various treatment groups of rats was alleviated to some extent, and the high-dose DYY group exhibited a better effect than the low-dose group (Fig. 8).

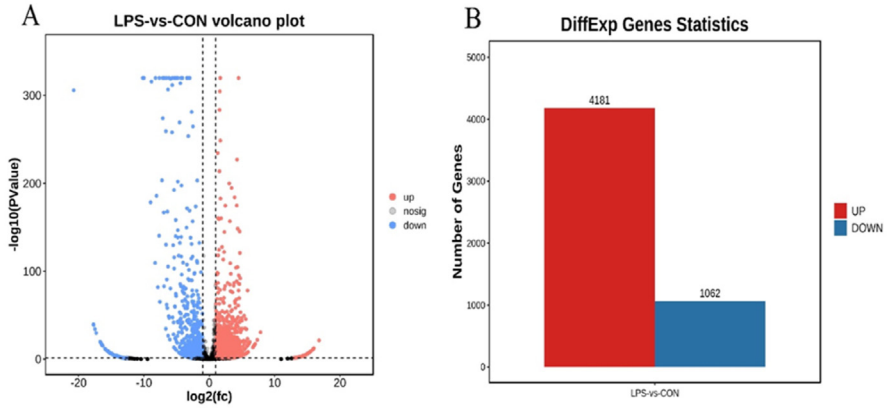

Fig. 2. Screening for common targets of DYY and ALI. A and B present volcano plots and bar graphs, respectively, illustrating the differential gene distribution in disease samples. Upregulated and downregulated genes are represented in red and sky blue, respectively, while black indicates no significant difference. Heatmap C displays the expression patterns of the top five differentially expressed genes between the ALI and normal groups. D presents a Venn diagram demonstrating the shared targets between the active components of DYY and ALI.

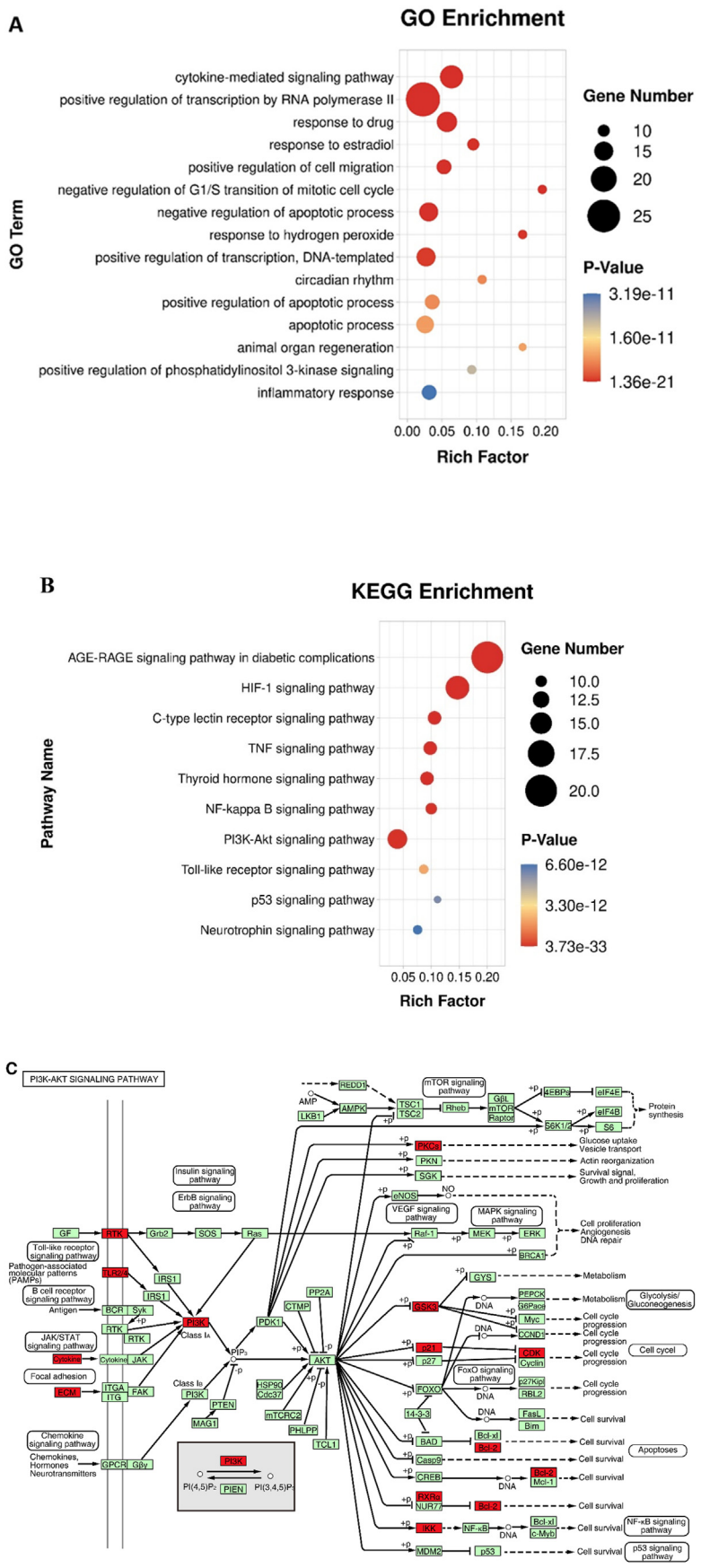

Fig. 3. Enrichment analysis of GO (A) and KEGG pathway (B) of ALI target genes in DYY therapy. Distribution of key targets in the most related signal pathway of PI3K/AKT (C). The key targets are represented by a red rectangle, while the light green represents the target genes associated with the pathway.

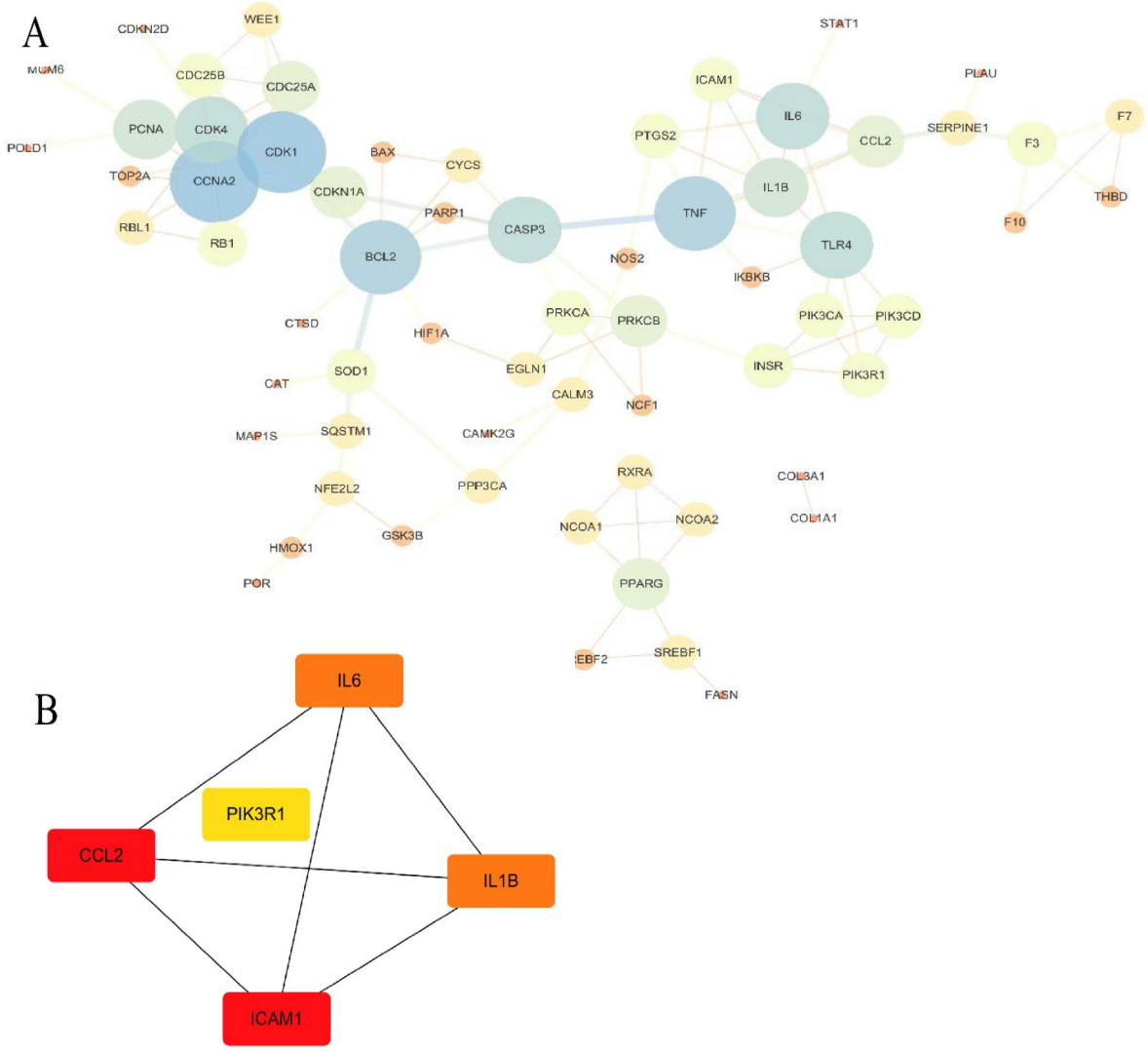

Fig. 4. Protein–protein interaction networks (A) and core target genes (B) of DYY for ALI treatment.

3.7.3. Effect of DYY on the PI3K/Akt/NF-κB signal pathway in lung tissue of ALI rats

In addition, the levels of phosphorylated PI3K, phosphorylated Akt, and phosphorylated NF-κBp65 in the lung tissue of ALI rats were detected, mainly focusing on the selected PI3K/Akt/NF-κB pathway (Fig. 9). The expression levels of phosphorylation PI3K, phosphorylation Akt, and phosphorylation NF-κBp65 in the lung tissue of the model group rats were significantly higher than those of the control group ($P < 0.01$). Compared with the model group, the phosphorylated expression of PI3K, AKT and NF-κB p65 decreased significantly in the DYY group (3.48, 6.96, and 13.92 g/kg, respectively). DYY has a protective effect on ALI rats related to the PI3K/AKT/NF-κB signal pathway.

3.7.4. Effects of DYY on inflammatory cells and inflammatory cytokines in BALF of rats

Experimental findings showed that the number of macrophages, lymphocytes and neutrophils in BALF of the model group was significantly higher than that of the control group, and the levels of IL-6, tumor necrosis factor-α and IL-1β were significantly increased. ($P < 0.01$). Surprisingly, it was observed that the treatment groups exhibited a significant reduction in the number of macrophages, lymphocytes, and neutrophils in BALF of each treatment group was significantly lower than that of the model group, along with a significant decrease in IL-6 levels ($P < 0.01$), as well as a significant decrease in TNF-α and IL-1β levels ($P < 0.01$) than those of the model group, as shown in Fig. 10.

4. Discussion

ALI is a clinically severe respiratory disease characterized by high incidence and mortality rates due to a series of pathological changes caused by lung tissue injury.[26,27] ALI is primarily characterized by excessive production of pro-inflammatory cytokines, apoptosis, and oxidative stress, which are often accompanied with the destruction of the alveolar endothelial cell barrier and neutrophil infiltration in the lung tissue. Alveolar macrophages and neutrophils play important roles in the pathogenesis of ALI.[28] Despite the existence of numerous treatment options, the current therapies primarily aim to alleviate the symptoms of the disease rather than effectively improving and/or reversing lung pathology or reducing mortality rates in patients with ALI. TCM has long been used as a clinical approach for treating ALI in China and has been proven to be effective and safe,[8,29] providing a new means for the multipoint treatment of ALI.

DYY was originally developed from human experience as a treatment strategy for acute respiratory diseases.[30] Experimental studies have provided evidence that specific constituents of DYY possess properties that mitigate pathological alterations in lung tissue, as well as exhibit anti-inflammatory and antioxidant effects.[10,31] Nevertheless, the precise bioactive chemical compounds and mechanisms by which DYY

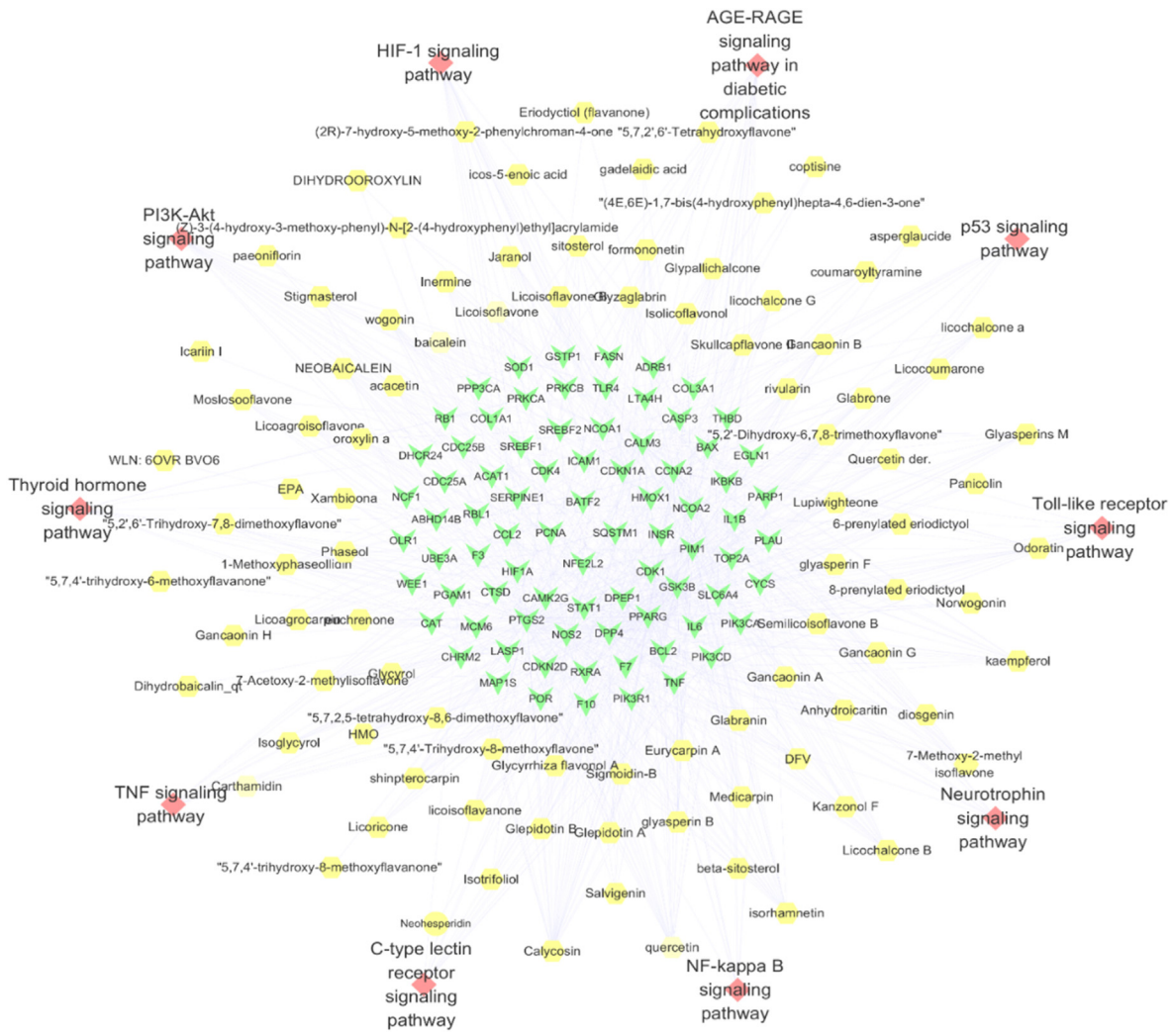

Fig. 5. Active component–target–pathway network of DYY for ALI treatment.

Table 1
Molecular docking binding energy of DYY core components and core targets.

Core component	Binding energy/(kJ·mol^{-1})				
	PIK3R1 (PDBID 2RD0)	CCL2 (PDBID 1DOK)	IL-1β (PDBID 1HIB)	IL-6 (PDBID 1ALU)	ICAM1 (PDBID 1D3L)
Calycosin	−3.6	−2.2	−5.7	−2.2	−0.5
quercetin	−14.4	−3.7	−16.6	−3.7	−0.6
isorhamnetin	−1.4	−6.1	−12	−3.3	−0.6
kaempferol	−5.9	−2.5	−12.5	−3.7	−0.7
Licochalcone B	−4.5	−2.5	−12.5	−3.6	−0.6

counteracts ALI remain undetermined. Consequently, we employed a combination of network pharmacology, the GEO chip strategy, and molecular docking technology to identify potential active ingredients and targets of DYY in ALI. Furthermore, we substantiated its comprehensive pharmacological effects and mechanisms through animal experimentation.

First, 94 active components of DYY were screened using the TCMSP database and literature search, and 260 corresponding targets were obtained. Then, 5243 ALI DEGs were obtained using the GEO dataset, and 81 intersection targets were obtained through them. Based on the degree values of compound-target-pathway network, five active ingredients of DYY were confirmed such as calycosin, quercetin, isorhamnetin, kaempferol, and licochalcone B, respectively. Pretreatment with quercetin effectively improved pathological changes in LPS-induced lung tissue by inhibiting the secretion of proinflammatory factors and reducing myeloperoxidase activity and malondialdehyde levels.[32] Isorhamnetin could significantly alleviate neutrophil infiltration and pulmonary edema and inhibit the secretion of inflammatory factors and phosphorylation of NF-κBp65.[33] Kaempferol treatment could inhibit the activation of NF-κB signaling pathway as well as reduce the oxidative damage and inflammatory process of lung tissue, thereby significantly reducing the W/D ratio and number of inflammatory cells in BALF of ALI mice and reducing the extent of lung tissue edema.[34] Licochalcone B inhibited LPS-induced ALI in mice and significantly improved oxidative stress and inflammatory markers.[35] These studies clearly demonstrated the therapeutic effects of the active ingredients in the compound prescription of TCM on ALI. To further clarify the mechanism of DYY in treating ALI, the GO analysis of intersection targets indicated that the active components in DYY may be involved in the bidirectional regulation and coordinated migration of cell inflammatory response and apoptosis. Combined with cell annotation and experimental verification results, DYY may act on lymphocytes, macrophages, and neutrophils to produce different biological functions, thereby exerting the therapeutic effects of treating ALI, mainly manifested as improvement in the lung wet/dry ratio and lung pathological damage. The KEGG analysis indicated that signaling pathways such as PI3K-Akt, TNF, and NF-κB may play a protective role in the treatment of ALI by DYY.

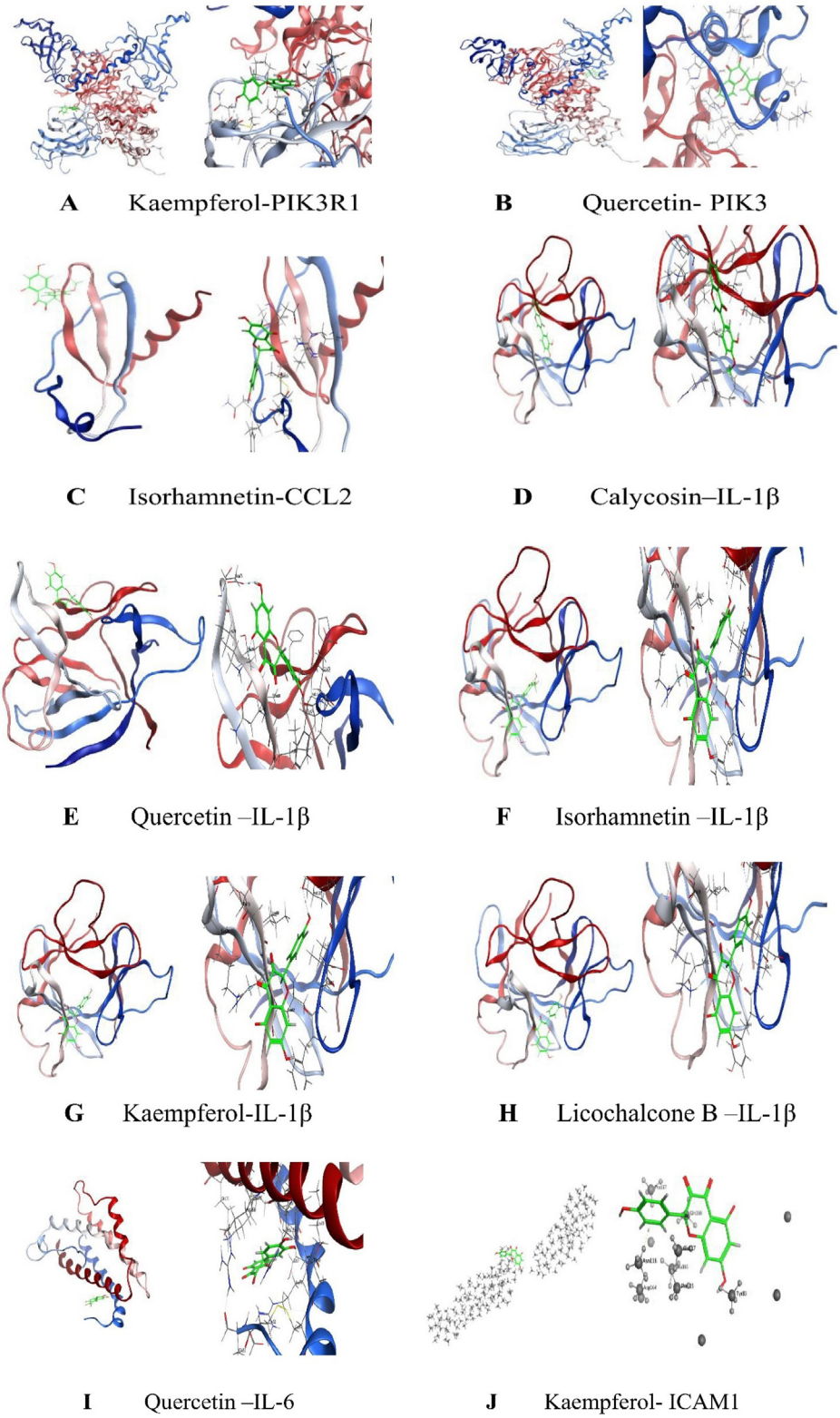

Fig. 6. Molecular docking patterns between main core components and core targets of DYY for ALI treatment. A: Kaempferol-PIK3R1. B: Quercetin-PIK3R1. C: Isorhamnetin-CCL2. D: Calycosin–IL-1β. E: Quercetin–IL-1β. F: Isorhamnetin–IL-1β. G: Kaempferol-IL-1β. H: Licochalcone B –IL-1β. I: Quercetin–IL-6. J: Kaempferol-ICAM1.

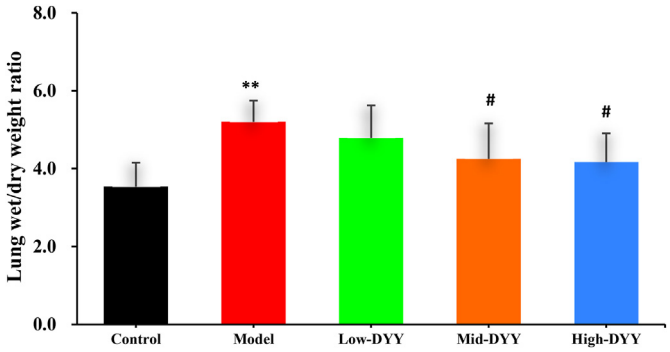

Fig. 7. Effects of DYY on pulmonary wet/dry weight ratio in rats with ALI rats ($x \pm s$, $n = 6$). Compared with the control group, $^{**}P < 0.01$; compared with the model group, $^{\#}P < 0.05$.

In addition, we also screened the core targets of DYY for ALI as follows: IL-6, IL-1β, PIK3R1, CCL2, and ICAM-1. These target genes are closely associated with ALI. Alveolar macrophages and epithelial cells may exert promoter-like effects in ALI. The excessive secretion of IL-1β can promote neutrophils and macrophages to gather in blood vessels and alveoli, subsequently leading to the impairment of vascular endothelial cells and alveolar epithelial cells, resulting in increased alveolar capillary permeability and pulmonary edema.[36] IL-1β also plays its role through downstream cytokines TNF-α and IL-6; TNF-α is an initiating factor produced and released by mononuclear macrophages and lymphocytes, which causes a "waterfall effect" after acting on neutrophils.[37,38] Lymphocytes are activated by abnormally elevated IL-6 levels, which in turn promotes the differentiation and infiltration of macrophages, leading to further aggravation of the inflammatory reaction.[39] A meta-study found has reported that ALI was closely related to significantly increased levels of IL-1β, IL-6, and TNF-α.[40] The results of molecular docking indicated that ICAM1 had the lowest binding affinity among the five target proteins. However, quercetin, kaempferol, and isorhamnetin had good binding abilities with PIK3R1, IL-1β, CCL2, and IL-6, indicating a high possibility of interaction between the components and targets.

Finally, in vivo experiments confirmed that DYY inhibited the increase in the lung W/D ratio induced by LPS in ALI rats and played a protective role in lung tissue by reducing pulmonary microvascular permeability, improving inflammatory cell infiltration, and alleviating LPS-induced lung edema. Furthermore, the regulatory effect of DYY on key signal pathways in lung tissue was further verified, and the expression levels of p-PI3K, *p*-Akt, and p–NF–κBp65 in DYY group were significantly decreased compared with the model group. Enzyme-linked immunoassay results revealed that compared with the model group, DYY significantly decreased the levels of pro-inflammatory cytokines TNF-α, IL-1β, and IL-6 in the BALF of model rats. Studies have demonstrated that in cells, when LPS binds to toll-like receptor 4 on the surface of macrophages, it activated PI3K and caused Akt to transfer from the cytoplasm to the cell membrane and phosphorylate. The activated Akt phosphorylated IKK, and *p*-IKK relieved the inhibition of IκB on NF-κB by

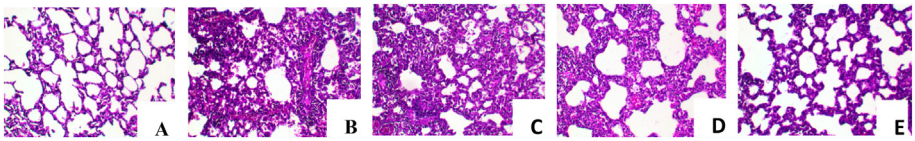

Fig. 8. Effects of DYY on histopathological changes of lung obtained from LPS-induced ALI rats of different groups. A: Control group; B: Model group; C: LPS + DYY (3.48 g/kg) group; D: LPS + DYY (6.96 g/kg) group; E: LPS + DYY (13.92 g/kg) group (hematoxylin and eosin E staining, magnification × 200).

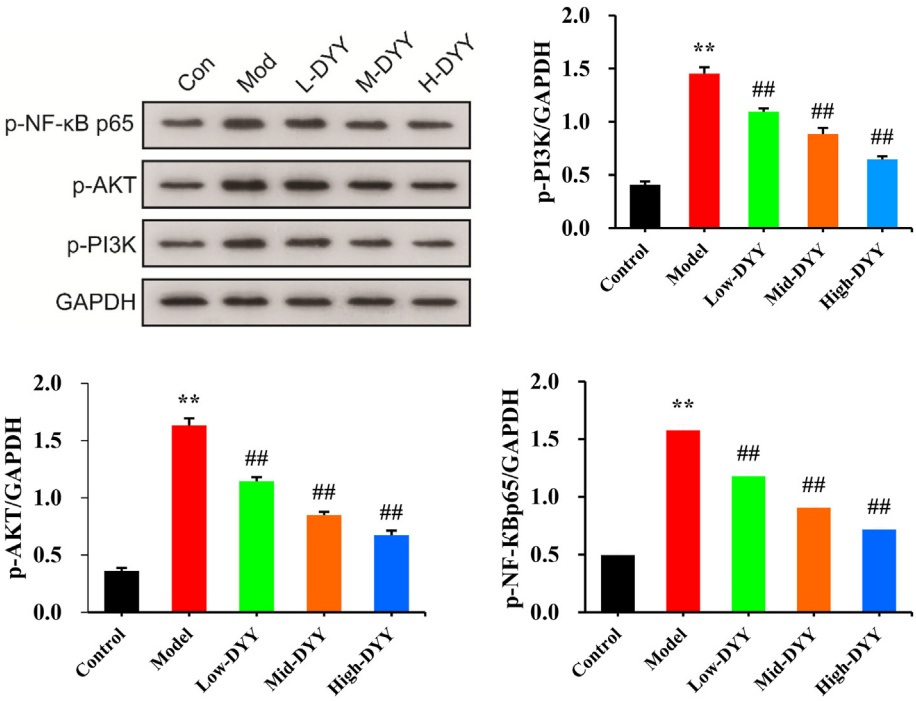

Fig. 9. DYY downregulated the protein levels of PI3K/Akt/NF-κB pathway. It mainly demonstrates the band and bar chart of the p-PI3K, *p*-AKT, and p–NF–κB p65 protein expressions. Compared with the control group: $^{**}P < 0.01$; compared with the model group: $^{\#\#}P < 0.01$. Data are represented as means ± standard deviations; $n = 3$ per group.

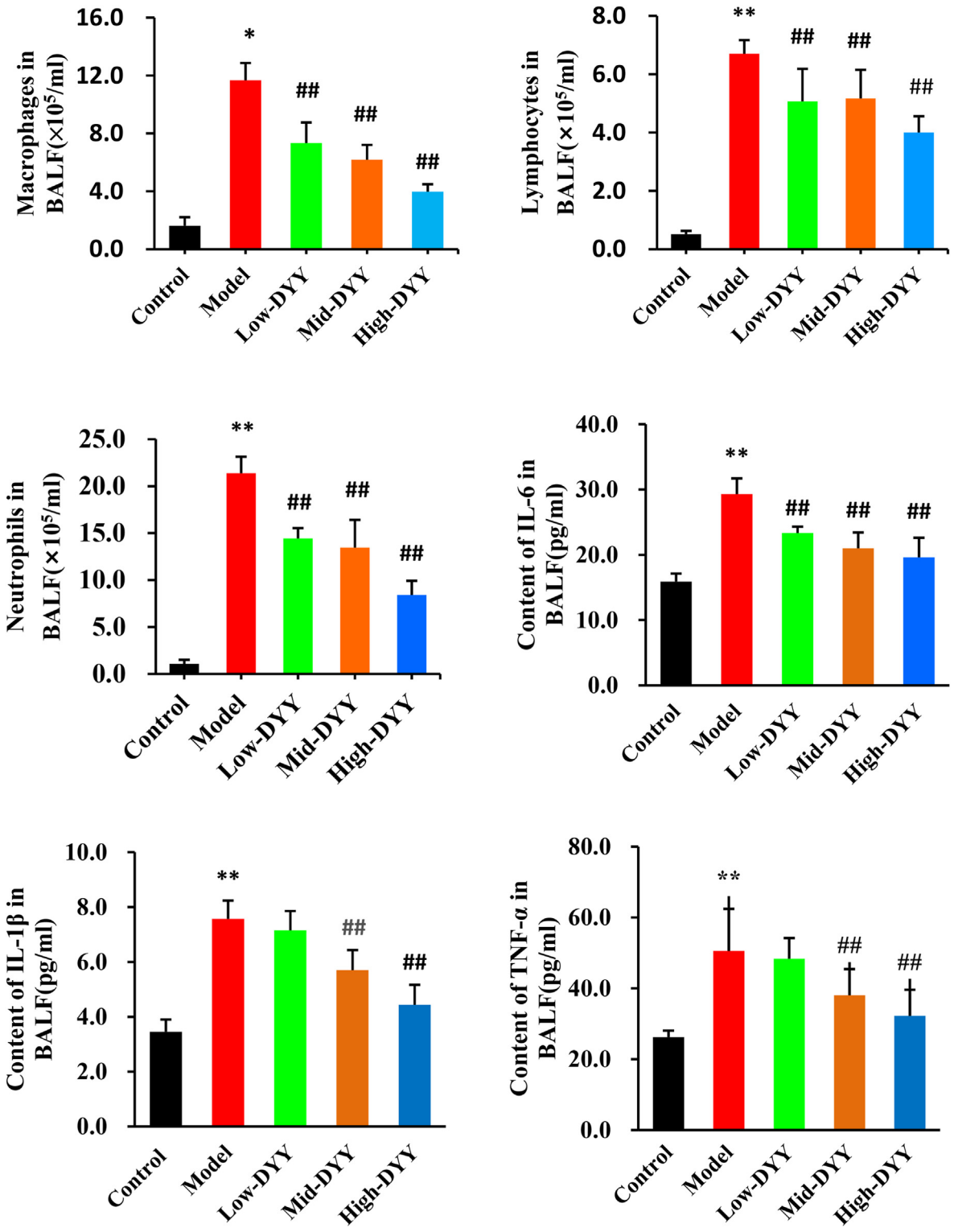

Fig. 10. Lipopolysaccharide-induced changes in macrophages, lymphocytes, neutrophils, and interleukin (IL)-6, tumor necrosis factor-α, IL-1β in bronchoalveolar lavage fluid (BALF) and inhibition of DYY compared with the control group, $^{**}P < 0.01$; compared with the model group, $^{\#\#}P < 0.01$.

phosphorylating IκB, and then phosphorylated NF-κB and translocated it to the nucleus. Since then, phosphorylated NF-κBp65 destroyed the integrity of allar capillaries by regulating the secretion of many pro-inflammatory cytokines such as TNF-α, IL-1β, and IL-6, and induced several monocytes-macrophages and neutrophils to gather in the lungs, aggravating inflammation and leading to pulmonary edema.[41,42] The results of this experiment are consistent with those of previous studies on inflammatory factors and pathological changes in lung tissue.

5. Conclusions

In this study, we employed a combination of network pharmacology and the Gene Expression Omnibus (GEO) database to forecast the primary bioactive compounds and potential targets of DYY in the

management of ALI. Furthermore, we have provided preliminary evidence elucidating the molecular mechanisms underlying its therapeutic action. These findings underscore the potential of DYY as a viable therapeutic agent for ALI. However, it is important to acknowledge the limitations of this study. Owing to the constraints imposed by the database information, there is a possibility of overlooking other active compounds, thereby compromising the representativeness of the analyzed components in relation to DYY. It is posited that the aforementioned shortcomings can be rectified in the future through the utilization of contemporary analytical methodologies, including chromatography-mass spectrometry, spectroscopy, and gene chip technology. Moreover, while the substantiation provided by molecular docking and in vivo experiments holds some persuasiveness, it remains insufficient. Consequently, the investigation into the correlation between syndrome and micro-level can be further expanded through the implementation of multi-omics approaches.

Funding

The present research was supported by Suzhou Science and Technology Bureau (serial number: SKJYD2021182).

Data availability statement

Datasets used and/or analyzed during the current study are available. It shall be provided by the corresponding author on reasonable request.

Ethics approval and consent to articipate

The Experimental Animal Welfare Ethics Committee (approval number 20221128) of Wuhan Optimal Biotechnology Co., Ltd. Granted approval for this study.

Patient consent for publication

Not applicable.

CRediT authorship contribution statement

Lei Zhang: Formal analysis. **Wei Zhu:** Formal analysis. **Zepeng Zhang:** Data curation. **Yu Huang:** Data curation.

Declaration of competing interest

The authors declare that they have no competing interests.

Acknowledgements

I would like to express my gratitude to Wuhan Optimal Biotechnology Co., Ltd. for providing the animal experimental equipment, facilities, and sample collection. Without their assistance, my research progress would have been greatly impeded. We also would like to thank Editage (www.editage.cn) for English language editing.

Appendix A. Supplementary data

Supplementary data to this article can be found online at https://doi.org/10.1016/j.jhip.2024.01.002.

References

1. Vohwinkel CU, Hoegl S, Eltzschig HK. Hypoxia signaling during acute lung injury. *J Appl Physiol*. 2015;119(10):1157–1163. https://doi.org/10.1152/japplphysiol.00226.2015.
2. Zheng L, Zhang Z, Song K, et al. Potential biomarkers for inflammatory response in acute lung injury. *Open Med*. 2022;17(1):1066–1076. https://doi.org/10.1515/med-2022-0491.
3. Standiford TJ, Ward PA. Therapeutic targeting of acute lung injury and acute respiratory distress syndrome. *Transl Res*. 2016;167(1):183–191. https://doi.org/10.1016/j.trsl.2015.04.015.
4. Ward PA. Oxidative stress: acute and progressive lung injury. *Ann N Y Acad Sci*. 2010;1203:53–59. https://doi.org/10.1111/j.1749-6632.2010.05552.x.
5. Kellner M, Noonepalle S, Lu Q, et al. ROS signaling in the pathogenesis of acute lung injury (ALI) and acute respiratory distress syndrome (ARDS). *Adv Exp Med Biol*. 2017;967:105–137. https://doi.org/10.1007/978-3-319-63245-2_8.
6. Mokrá D. Acute lung injury-from pathophysiology to treatment. *Physiol Res*. 2020;69(Suppl 3):S353–S366. https://doi.org/10.33549/physiolres.934602.
7. Ding Z, Zhong R, Xia T, et al. Advances in research into the mechanisms of Chinese Materia Medica against acute lung injury. *Biomed Pharmacother*. 2020;122:109706. https://doi.org/10.1016/j.biopha.2019.109706.
8. Wang Q, Zhu H, Li M, et al. Efficacy and safety of Qingfei Paidu Decoction for treating COVID-19: a systematic review and meta-analysis. *Front Pharmacol*. 2021;12:688857. https://doi.org/10.3389/fphar.2021.688857.
9. Millar MW, Fazal F, Rahman A. Therapeutic targeting of NF-κB in acute lung injury: a double-edged sword. *Cells*. 2022;11(20):3317. https://doi.org/10.3390/cells11203317.
10. Yang Y, Chen J, Ren H, et al. Protective effect of the eluting fraction of Da-Yuan-Yin decoction on acute lung injury. *Alternative Ther Health Med*. 2023;29(5):242–254.
11. Ni Y, Jiang T, Cheng Q, et al. Protective effect of magnolol on lipopolysaccharide-induced acute lung injury in mice. *Inflammation*. 2012;35(6):1860–1866. https://doi.org/10.1007/s10753-012-9507-9.
12. Tsai CL, Lin Y, Wang H, et al. Baicalein, an active component of *Scutellaria baicalensis*, protects against lipopolysaccharide-induced acute lung injury in rats. *J Ethnopharmacol*. 2014;153(1):197–206. https://doi.org/10.1016/j.jep.2014.02.010.
13. Lee SA, Lee SH, Kim JY, et al. Effects of glycyrrhizin on lipopolysaccharide-induced acute lung injury in a mouse model. *J Thorac Dis*. 2019;11(4):1287–1302.
14. Zhou B, Weng G, Huang Z, et al. Arctiin prevents LPS-induced acute lung injury via inhibition of PI3K/AKT signaling pathway in mice. *Inflammation*. 2018;41(6):2129–2135. https://doi.org/10.1007/s10753-018-0856-x.
15. Wang K, Miao X, Kong F, et al. Integrating network pharmacology and experimental verification to explore the mechanism of effect of Zuojin Pills in pancreatic cancer treatment. *Drug Des Dev Ther*. 2021;15:3749–3764. https://doi.org/10.2147/DDDT.S323360.
16. Li X, Liu Z, Liao J, et al. Network pharmacology approaches for research of Traditional Chinese Medicines. *Chin J Nat Med*. 2023;21(5):323–332. https://doi.org/10.1016/S1875-5364(23)60429-7.
17. Zhang X, Ding C, Zhao Z. Identification of diagnostic molecules and potential therapeutic agents for atopic dermatitis by single-cell RNA sequencing combined with a systematic computing framework that integrates network pharmacology. *Funct Integr Genomics*. 2023;23(2):95. https://doi.org/10.1007/s10142-023-01005-3.
18. Holloman BL, Cannon A, Wilson K, et al. Aryl hydrocarbon receptor activation ameliorates acute respiratory distress syndrome through regulation of Th17 and Th22 cells in the lungs. *mBio*. 2023;14(2):e0313722. https://doi.org/10.1128/mbio.03137-22.
19. Sinha D, Kumar A, Kumar H, et al. dropClust: efficient clustering of ultra-large scRNA-seq data. *Nucleic Acids Res*. 2018;46(6):e36. https://doi.org/10.1093/nar/gky007.
20. Liang B, Xiang Y, Zhang X, et al. Systematic pharmacology and GEO database mining revealed the therapeutic mechanism of xuefu zhuyu decoration for atherosclerosis cardiovascular disease. *Front Cardiovasc Med*. 2020;7:592201. https://doi.org/10.3389/fcvm.2020.592201.
21. Guo N, Xu Y, Cao Z. Absinthin attenuates LPS-induced ALI through MIP-1α-mediated inflammatory cell infiltration. *Exp Lung Res*. 2015;41(9):514–524. https://doi.org/10.3109/01902148.2015.1093566.
22. Shi Z, Yu C, Wu Z, et al. The effect of FTY720 at different doses and time-points on LPS-induced acute lung injury in rats. *Int Immunopharm*. 2021;99:107972. https://doi.org/10.1016/j.intimp.2021.107972.
23. Zeng Y, Zhao H, Zhang T, et al. Lung-protective effect of Punicalagin on LPS-induced acute lung injury in mice. *Biosci Rep*. 2022;42(1):BSR20212196. https://doi.org/10.1042/BSR20212196.
24. Fu K, Piao T, Wang M, et al. Protective effect of catalpol on lipopolysaccharide-induced acute lung injury in mice. Int *Immunopharmacol*. 2014;23(2):400–406. https://doi.org/10.1016/j.intimp.2014.07.011.
25. Dhlamini Q, Wang W, Feng G, et al. FGF1 alleviates LPS-induced acute lung injury via suppression of inflammation and oxidative stress. *Mol Med*. 2022;28(1):73. https://doi.org/10.1186/s10020-022-00502-8.
26. Butt Y, Kurdowska A, Allen TC. Acute lung injury: a clinical and molecular review. *Arch Pathol Lab Med*. 2016;140(4):345–350. https://doi.org/10.5858/arpa.2015-0519-RA.
27. Liu X, Zhang J, Xie W. The role of ferroptosis in acute lung injury. *Mol Cell Biochem*. 2022;477(5):1453–1461. https://doi.org/10.1007/s11010-021-04327-7.
28. Hsieh PC, Wu Y, Yang M, et al. Deciphering the role of damage-associated molecular patterns and inflammatory responses in acute lung injury. *Life Sci*. 2022;305:120782. https://doi.org/10.1016/j.lfs.2022.120782.
29. Diao Y, Ding Q, Xu G, et al. Qingfei litan decoction against acute lung injury/acute respiratory distress syndrome: the potential roles of anti-inflammatory and anti-oxidative effects. *Front Pharmacol*. 2022;13:857502. https://doi.org/10.3389/fphar.2022.857502.
30. Wang Y, Yuan Y, Wang W, et al. Mechanisms underlying the therapeutic effects of Qingfeiyin in treating acute lung injury based on GEO datasets, network

pharmacology and molecular docking. *Comput Biol Med*. 2022;145:105454. https://doi.org/10.1016/j.compbiomed.2022.105454.
31. Guo L, Yang Y, Yuan J, et al. Da-Yuan-Yin decoction polyphenol fraction attenuates acute lung injury induced by lipopolysaccharide. *Pharm Biol*. 2023;61(1):228–240. https://doi.org/10.1080/13880209.2023.2166085.
32. Wang L, Chen J, Wang B, et al. Protective effect of quercetin on lipopolysaccharide-induced acute lung injury in mice by inhibiting inflammatory cell influx. *Exp Biol Med*. 2014;239(12):1653–1662. https://doi.org/10.1177/1535370214537743.
33. Chi G, Zhong W, Liu Y, et al. Isorhamnetin protects mice from lipopolysaccharide-induced acute lung injury via the inhibition of inflammatory responses. *Inflamm Res*. 2016;65(1):33–41. https://doi.org/10.1007/s00011-015-0887-9.
34. Chen X, Yang X, Liu T, et al. Kaempferol regulates MAPKs and NF-κB signaling pathways to attenuate LPS-induced acute lung injury in mice. *Int Immunopharm*. 2012;14(2):209–216. https://doi.org/10.1016/j.intimp.2012.07.007.
35. Huang J, Zhu Y, Li S, et al. Licochalcone B confers protective effects against LPS-Induced acute lung injury in cells and mice through the Keap1/Nrf2 pathway. *Redox Rep*. 2023;28(1):2243423. https://doi.org/10.1080/13510002.2023.2243423.
36. Yoshinar D, Takeyoshi I, Koibuchi Y, et al. Effects of a dual inhibitor of tumor necrosis factor-α and interleukin-1 on lipopolysaccharide-induced lung injury in rats: Involvement of the p38 mitogen-activated protein kinase pathway. *Crit Care Med*. 2001;29(3):628–634. https://doi.org/10.1097/00003246-200103000-00029.
37. Susantitaphong P, Perianayagam MC, Tighiouart H, et al. Tumor necrosis factor alpha promoter polymorphism and severity of acute kidney injury. *Nephron Clin Pract*. 2013;123(1-2):67–73. https://doi.org/10.1159/000351684.
38. Wan S, LeClerc JL, Vincent JL. Cytokine responses to cardiopulmonary bypass: lessons learned from cardiac transplantation. *Ann Thorac Surg*. 1997;1:269–276. https://doi.org/10.1016/s0003-4975(96)00931-9.
39. Choussat R, Montalescot G, Collet J, et al. Effect of prior exposure to Chlamydia pneumoniae, Helicobacter pylori, or cytomegalovirus on the degree of inflammation and one-year prognosis of patients with unstable angina pectoris or non-Q-wave acute myocardial infarction. *Am J Cardiol*. 2000;86(4):379–384. https://doi.org/10.1016/s0002-9149(00)00950-4.
40. Liu Z, Liu D, Wang Z, et al. Association between inflammatory biomarkers and acute respiratory distress syndrome or acute lung injury risk : a systematic review and meta-analysis. *Wien Klin Wochenschr*. 2022;134(1-2):24–38. https://doi.org/10.1007/s00508-021-01971-3.
41. Ge X, Meng X, Fei D, et al. Lycorine attenuates lipopolysaccharide-induced acute lung injury through the HMGB1/TLRs/NF-κB pathway. *3 Biotech*. 2020;10(8):369. https://doi.org/10.1007/s13205-020-02364-5.
42. Zhao M, Li C, Shen F, et al. Naringenin ameliorates LPS-induced acute lung injury through its anti-oxidative and anti-inflammatory activity and by inhibition of the PI3K/AKT pathway. *Exp Ther Med*. 2017;14(3):2228–2234. https://doi.org/10.3892/etm.2017.4772.